*International Journal of Geology, Earth & Environmental Sciences ISSN: 2277-2081*
*An Open Access, Online International Journal Available at http://www.cibtech.org/jgee.htm*
*2022 Vol. 12, pp. 31-56/Karl*
***Research Article***

# ENVIRONMENTAL CHANGES IN MANILA BAY

***Karl H. Szekielda**
*International Faculty, Ateneo de Manila University*
*Department of Environmental Science*
**Author for Correspondence: kszekielda@ateneo.edu*

**ABSTRACT**
The climate of Manila Bay is exposed to the northeast monsoon that dominates from November to January, the southeasterly monsoon from February to May, and from June to September, the bay is exposed to southwesterly winds. The basic characteristics of the bay during the seasons are analyzed over two decades with the normalized fluorescence line height (NFLH), sea surface temperature (SST) and selected spectral wavelengths. The NFLH is not necessarily correlated with remote sensing reflectance at different wavelenghts as well as with temperature. The season February to May shows the lowest NFLH coinciding with reduced river discharge of the Pampanga and Pasig Rivers. During the southwest monsoon, from June to September, the fluorescence increases but is still comparably low. The season during which the Pasig and Pampanga Rivers start to increase their discharge shows increasing NFLH values in August in the eastern part of the bay. Minimum NFLH has been recognized every year in February/March, and decrease of NFLH continues until April. Towards May, an increase of NFLH is observed at the eastern part of the bay when the transition time from southeasterly winds to southwesterly winds emerges. The appearance of NFLH minimum in the center of the bay is a characteristic feature that is also recognized in zonal longitudal NFLH. Changes observed with NFLH are also detected with remote sensing reflectance ($R_{rs}$) at various wavelengths. Linear regressions and polynomial fits show changes that correspond to the values and time frame of global change events with an increase of remote sensing reflectance. Based on linear regressions, the highest increase is found at $R_{rs}$ 0.412µm and 0.443µm of around 30%. At $R_{rs}$ 0.667µm, close to the second absorption band of chlorophyll, the increase is about 20% and at $R_{rs}$ 0.555µm, an estimated increase of about 10%. An approximation for chlorophyll changes made with fluorescence measurements show a change of 0.009 mg chlorophyll $y^{-1}$. SST distribution in the bay ranges between $27^0$ C and $33^0$ C and linear regression shows SST increase of about $0.028^0$C $y^{-1}$ that is similar to the range of sea surface temperature around the Philippine coastal water. Forecasting shows that by 2035, major warming will be during the period of southwest winds when the surface circulation of the bay is in anticyclonic mode while minimum warming can be foreseen to appear especially during the months of southeast winds when cyclonic movement in the bay persists.

***Key words:*** *Manila Bay, Spatial-Temporal Change Rates, Temperature Increase, Eutrophication*

## INTRODUCTION
As an archipelago, the Philippines is enormously susceptible to the impacts of climate change. It shows a trend of increase averaged temperature of 0.65°C from 1951–2010, with highest increases in northern and southern parts of the Philippine islands, and sea level increase is estimated to be about 0.15 meters since 1940. The effect of those changes is manifested through increased frequency and severity of natural disasters, and environmental degradation. For instance, an increased frequency of cyclones during El Niño years was observed, and sea surface temperatures increased by 0.6° to 1°C since 1910, with most significant warming observed after the 1970s (USAID, 2017).
In general, the Philippines follow the global trend in ocean temperature-increase that shows an increase of about $0.5^0$C within two decades. In the average, the highest rate in sea surface temperature increase around the Philippines is observed for the June to August season with an estimated value of $0.036^0$ C $y^{-1}$ and lowest rate is observed for the December to February season at about $0.027^0$ C $y^{-1}$. By using estimates

for 2020 and 2050, it can be projected that within thirty years, an additional temperature increase of $1.8^0$ C can be expected in Philippine coastal waters (Szekielda and Guzman, 2021).

Temperature increase and changes of marine productivity are observed globally, and it is recognized that the marine ecosystem is in decline (Sathyendranath *et al.*, 2019; Boyce *et al.*, 2010, Behrenfeld *et al.*, 2006). On the other hand, observations in the Southern Ocean indicate that there is a significant increase in nutrients that does not seem to affect significantly the phytoplankton population (Rousseau and Gregg, 2015). This raises the question of how far regional and local marine ecosystems respond to global change and, in particular, to unusual ocean temperature increases that have been documented for large ocean regions (Roxy *et al.*, 2019) and on a regional level (Szekielda, 2020b). Globally, surface temperatures of the oceans to a depth of about 700 meters has been warmed at a rate of about 0.11°C, 0.07°C and 0.05°C per decade for the Indian, Atlantic and Pacific Oceans, respectively (Hoegh-Guldberg *et al.*, 2018). On a local scale, substantial fluctuations can appear in chlorophyll concentrations and increasing temperature may be a cause for the reduction in primary productivity. For instance, there is evidence that the upwelling system in the NW Indian Ocean has shown significant modifications (Szekielda, 2020a). However, the observed variability may also be a result of fluctuations with long periodicity, and random changes may occur over longer time frames as well. Studies in the South China Sea (Szekielda, 2020b) show the probability that superimposed to the seasonal variations in temperature, salinity and chlorophyll, are inter-annual variations that can be attributed to ENSO cycles, and are therefore most probably related to large changes in atmospheric circulation.

Based on these observations, it is of interest to identify changes that may appear at the local level such as the Manila Bay and the adjacent coastal region. The main environmental driver in the Manila region is the population and its dynamic that is related to the emission of byproducts from production and consumption. This makes it imperative to estimate the level of environmental changes that can be anticipated for the next decades. Manila Bay is located in the western part of Luzon between 14.23° and 14.87°N and 120.53° and 121.03°E. It is bounded by Cavite and Metro Manila on the east, Bulacan and Pampanga on the north, and Bataan on the west and northwest. The climate of the bay follows the major wind regimes namely the northeast monsoon that dominates from November to January and the southeasterly monsoon from February to May, and from June to September, the bay is exposed to southwesterly winds. The dry season in the bay region is from November to May, and the wet season from June to September, while August has on the average the highest, and February has the lowest rainfall. The 190 km coastline of the bay covers the provinces of Cavite, Metro Manila, Bulacan, Pampanga, and Bataan. The bathymetry of the bay has a slight slope and the basin has an average depth of about 17 m (PEMSEA, 2007). The bay receives fresh water from 26 catchment zones (Jacinto *et al.*, 2011). Water exchange between the bay and the coastal ocean takes place through the entrance that is about 19 km wide and is flanked by the islands Corregidor and Caballo. The annual average volume of freshwater discharge into the bay is estimated to be about 6.6 million $m^3$ with low discharge from March to May and high freshwater inflow during October to November. The Pampanga and Pasig Rivers are the major contributors of fresh water influx into the bay (Jacinto et al. 2006a). Major contributor is the Pasig River that connects Manila Bay and Laguna Bay and runs across Metro

Manila before discharging into the Manila Bay from March to May at about 12 $m^3$ $sec^{-1}$, and from October to November, it delivers about 275 $m^3$ $sec^{-1}$ (Gorme *et al.*, 2010). Runoff from the river system into bay water contains septic waste that is directly discharged into the river during heavy rains as well as sludge with high amounts of oil and grease coming from nearby populated areas. Water quality varies with meteorological seasons and generally almost no dissolved oxygen is present during low water discharge while oxygen levels can be higher than 5 mg/l during the rainy season (Clemente, 2020). River discharge also transports high loads of suspended matter and dissolved nutrients that are carried from about 17,000 km$^2$-drainage areas. The Pasic River delivers especially ammonium in high concentration, and the river seems to be the main source of nutrient input to the bay (Chang *et al.*, 2009).

The bay is exposed to intense human settlement, resource extraction and industrial development. This resulted over the years in deterioration of the coastal environment as mangroves around Manila were lost and the bay water quality deteriorated. The enormous impact of industrial fallout into the bay is shown with the load of heavy metals as Pb, Cd, and Hg concentrations in the bay occasionally exceeding the permissible limits especially with regards to the lead concentration (Sy *et al.*, 2017).

A major environmental concern in the Philippines is the severe impact of pollution in particular in Manila Bay and along the nearby coastal area that originates from agricultural practices, and discharge of untreated sewage. Eutrophication in the bay is the result from this high discharge of nutrients (Reyes and Bedoya, 2008, Chang *et al.*, 2009, Poquita-Du and Todd, 2015, Sy *et al.*, 2017, Vergara *et al.*, 2017, Borja *et al.*, 2019). The immense discharge of effluent from households and industries lead to occasional development of harmful plankton blooms and occurrence of hydrogen sulfide at the lower depths. As a result, red tides and outbreak of harmful toxic algal blooms in coastal waters are observed with high frequency (Wang et al. 2008), and nutrient levels and oxygen consumptions are indicators for environmental degradation (Chang *et al.,* 2009, Velasquez and Jacinto, 1995, Jacinto *et al.,* 2011). Preliminary comparison of remote sensing-derived chlorophyll *a* concentration and sea surface temperature by Poniente and Santos (2017) showed that high concentration of chlorophyll was generally found in the eastern and southwestern parts of the bay and sea surface temperature can be high, reaching more than 30 °C, but by comparison, the lower side of the bay has lower temperature. Elevated chlorophyll concentrations in Manila Bay are the effect of extremely high nutrient release into the bay but may not decrease with better sewage treatment because of the high population growth and socio-economic development that would counter partially the improvement in water quality. In the past, outbreaks of red tides and other harmful algal blooms were documented with a trend toward increasing frequency in Manila Bay (Tirado and Bedoya, 2008; Wang *et al.*, 2008; Soto *et al.*, 2015).

A large source of nutrient input to coastal waters is derived from fertilizers that are not efficiently absorbed during agricultural use. There is a steady increase of consumption of fertilizers in the Philippines but the increase is not proportional to the yield and consequently, the non-converted fertilizers are washed into the hydrological system with its destination to the coastal region. At present, eutrophication in the Manila Bay region appears to decline and this is possibly an outcome of integrated coastal zone management around Manila Bay that contributed to the decline of nitrate and phosphate concentrations in Manila Bay as evidenced with an inventory of nutrient concentrations in the bay (Jacinto *et al.,* 2006b). The complexity in the environment of the bay is shown with observations that salinity, temperature, dissolved oxygen, phosphate and nitrate have positive correlation with zooplankton copepods, and that isolated ecosystems are observed in high concentrations in the eastern and southern part of the bay (Jose *et al.*, 2015).

Manila Bay hydrodynamics are controlled by the combined effect of wind stress that changes dramatically with the varying monsoon seasons, freshwater discharge, surface temperature changes from incident radiation and tides. The bay has typical estuarine flow although the exchange of water from the bay with ocean water is restricted during flood and high tide, but it is accelerated during ebb and low tides (Pokavanich and Nadaoka, 2006). The surface circulation is also reflected in the temperature distribution that shows warmer water along the shallower north to southwest bank where also low salinity is found. Modeled currents from the combined effects of ocean tide and uniformed wind showed that the overall circulation in the bay is based on tide and wind induced currents. The tidal forces in the bay are strongest at the mouth but decrease towards the head of the bay. As shown in Figure 1, wind-driven forcing initiates two gyres that change their rotation according to the prevailing wind direction (De Las Alas and Sodusta, 1985) although the dominance of the wind-driven component is present only in part of the near-coastal water (Villanoy and Martin, 1997). Cyclonic movement of the surface is observed during the seasons with southeast and northeast direction while anticyclonic circulation is present during the southwest monsoon.

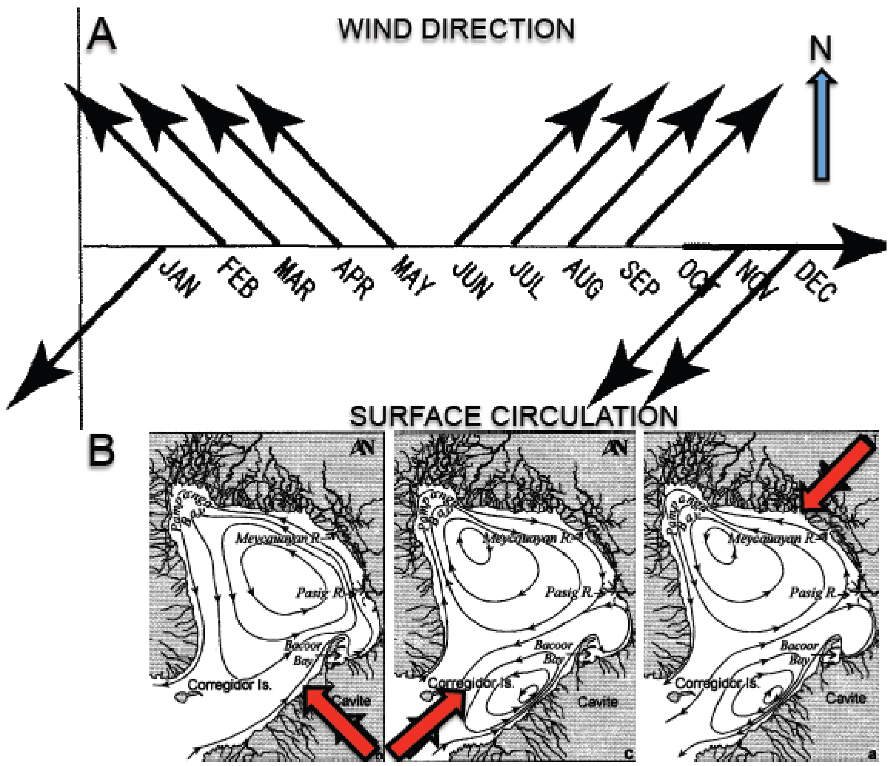


**Figure 1: A: Wind direction at Manila Bay; B: Wind-driven surface circulation during the different monsoon seasons. Modified from De Las Alas and Sodusta (1985).**

In response to changing rates of precipitation and river discharge into the bay, highest salinities are observed in November and lowest is observed from May to July that falls together with the maximum water temperature. The bay undergoes occasional stratification that is mainly determined by salinity and less by temperature (Sy *et al.*, 2017). Average surface salinity is around 32.6 psu but undergoes seasonal fluctuations that are a result of river discharge, tidal action and seasonal fluctuation in wind stress (Jacinto *et al.*, 2006b). The major contribution of freshwater is derived from the catchments areas of the Pampanga and Pasig rivers. Submarine ground water also contributes to the nutrient budget in the bay and the quantity of discharged dissolved inorganic nitrogen by groundwater is comparable in magnitude to fluxes from each of the two major rivers that drain into Manila Bay (Taniguchi *et al.*, 2008). Based on salinity distribution, the bay water is well mixed although lower salinities are found in the vicinity to the coast whereas maximum salinity is observed in the near- bottom waters and close to the entrance of the bay.
The following study aims to address the impact of global change at the local level with sea surface temperature and fluorescence intensity. The present satellite data set covers a time frame of decades and permits to extract environmental changes at different time periods that are close to climatic processes. The study therefore elaborates with remote sensing data trends in temperature increase and related changes in Manila Bay and aims to document possible spatial-temporal changes at different time scales. The first part considers spectral signatures and temperature in form of image maps and describes averaged environmental conditions at various wavelengths. The second part shows the analysis of time series to extract temporal changes that are on the time-scale of global change events. The third part presents quantitative information with the aim to estimate the progression of the environmental changes in Manila Bay up to 2035.

**MATERIALS AND METHODS**

*The test site*

Manila Bay is shown in Figure 2 with the selected area in the center of the bay. The density of data at 4km-resolution in the selected box in Manila Bay leads to a total of 36 grid cells, each consisting of the averaged values of the original 1km-resolution data.

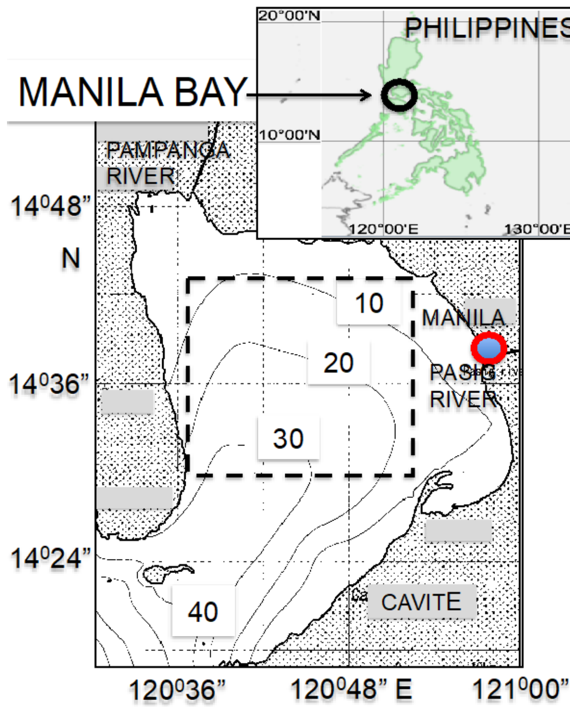


**Figure 2: Manila Bay, Philippines and its bathymetry in meters. The square indicates the test site; the discharge locations of the Pasig and Pampanga Rivers are included.**

The selected area is influenced by the effluents of the Pampanga in the northwest and the Pasig Rivers along the east flank of the bay. The selection of the central part of the bay considers the 4km-resolution of the data but also excludes partly extreme localized events such as direct freshwater discharge and plankton blooms close to the shore. It can be assumed that in this selected part of the bay, currents have accomplished major mixing between ocean and bay water. Remotely sensed data were accessed from the System for Multidisciplinary Research and Applications (NASA Giovanni) for the analysis of remote sensing data (Acker and Leptoukh, 2007, Giovanni User Guide" version 1.1) httpd://Giovanni.gsfc.nasa.gov/). The data used from Giovanni are based on the MODIS instrument that has 36 spectral bands between 0.405 and 14.385 µm. The data are displayed in different formats as time-series and averaged maps and were processed after downloading as CSV file. For time-dependent events, the animation service in Giovanni was used and interannual grouping of the data was selected for meteorological seasons December to February, March to May, June to July and September to October. Time series used in this study are based on calculating spatial averages over the study area. Hovmöller plots were averaged over latitude and longitude for the purpose to identifying with two-dimensional color graphs possible changes. Smoothing was applied and the same color palette of inverted spectral division of ten was applied to all stretching and color annotations.

In addition to SST, remote sensing reflectance was used at specific spectral bands that coincide with major absorption and reflection properties of constituents in seawater. In particular, the longer wavelengths close to the second absorption band of chlorophyll are suited to derive information on concentrations of biomass, if proper empirical factors are applied. As shown in Figure 3, the comparison of chlorophyll estimates in bay water with fluorescence data shows a rather low correlation. In order to characterize an equivalent of biomass, preference was given to fluorescence measurements because in coastal waters, the algorithm for chlorophyll becomes uncertain due to interference by other non-living material that is either present in particulate or dissolved forms (Hu and Feng, 2016).

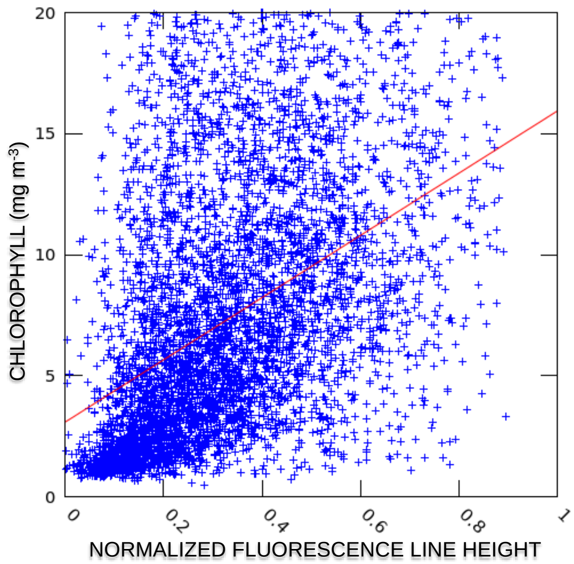


**Figure 3: Scatter diagram based on 5521 measurements July 2002 to December 2021 for chlorophyll concentrations in mg $m^{-3}$ and normalized fluorescence line height (NFLH) in mW $cm^{-2}$ $\mu m^{-1}$ $sr^{-1}$; R= 0.46.**

The estimate of fluorescence is based on chlorophyll fluorescence emission at 0.678µm. After atmospheric corrections, the residual oceanic component of the fluorescence also contains fluorescence from backscattered and Raman scattered sunlight that are accounted for by calculating the 0.678µm baseline radiance through linear interpolation of radiances measured at 0.667µm and 0.748µm. Subtraction of this baseline from the 0.678µm signal yields the fluorescence line height product (Behrenfeld *et al.*, 2009). In Giovanni, the final fluorescence values are available without requiring further processing.

The normalized fluorescence line height (NFLH) is an indicator for the solar stimulated chlorophyll fluorescence in phytoplankton because the absorption peak at longer wavelengths is mainly associated with chlorophyll, and the NFLH removes to a high degree the spectral interference of colored particulate and dissolved organic and non-algal matter. However, effects on the line height values are variations in the absolute cellular pigment concentration and relative cellular pigment composition induced by physiological responses to light history, nutrient status and taxonomic variability in pigment composition (Roesler and Barnard, 2013). In general, fluorescence line height measurements avoid some of the major impact of other optically active components in the water and serve as an indicator for plankton bloom conditions at the surface.

Some spectral bands in atmospherically corrected reflectance measurement, referred to as remote sensing reflectance $R_{rs}$, are used to diagnose the presence of specific absorbers or reflecting substances. Figure 4 demonstrates the principle of image interpretation as it relates to the spectral response of bay water, and shows that selecting the proper channel according to the desired spectral target, specific patch recognition can be achieved to identify temporal and spatial changes in connection with SST.

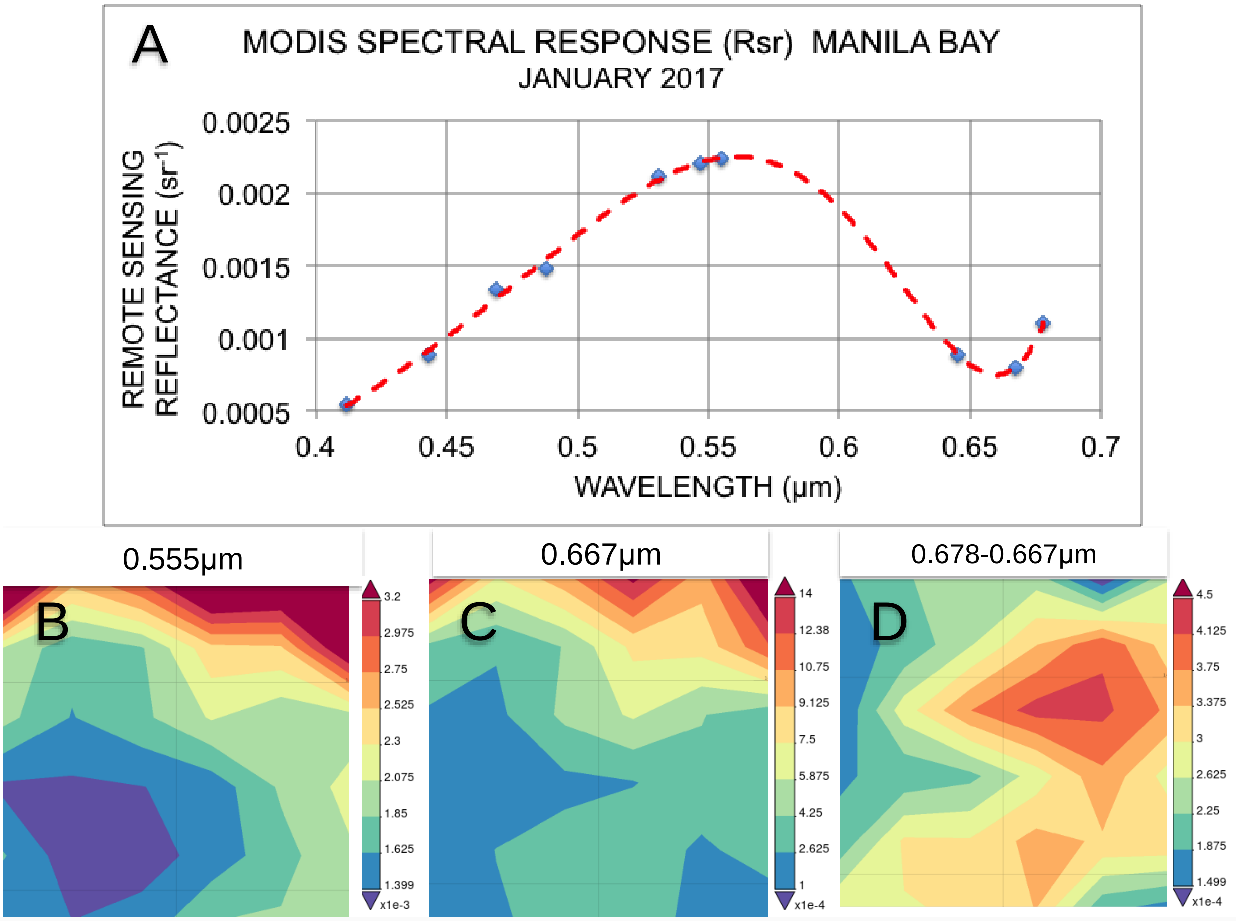


**Figure 4: Spectral performance of the MODIS channels over Manila Bay based on monthly averaged data for January 2017. A: Reconstructed channel response of remote sensing reflectance data. Remote-sensing reflectance is defined as the ratio of the water-leaving radiance to the incident sky irradiance $R_{rs} = L_w / E_d$, and the units are $sr^{-1}$. The curve is based on a polynomial fit and is included for visualizing the spectral location of the different bands and does not represent an actual reflectance spectrum. B: Reflectance map of Manila Bay at wavelength 0.555µm; C: Reflectance map at wavelength 0.667µm. D: Reflectance map based on the difference of wavelengths at 0.678µm and 0.667µm.**

Limited ship measurements allowed a qualitative comparison of patchiness in the distribution of temperature and fluorescence as recognized with GIOVANNI data. A comparison was done from aboard ship of single surface samples of chlorophyll measurements and monthly averaged fluorescence data as shown in Figure 5 that gives a qualitative agreement in the recognition of patchiness with high concentrations of chlorophyll. Linear regression of ship and NFHL values allowed an estimate where chlorophyll = 4.7255x - 0.2994 and x is the NFLH.

***Research Article***

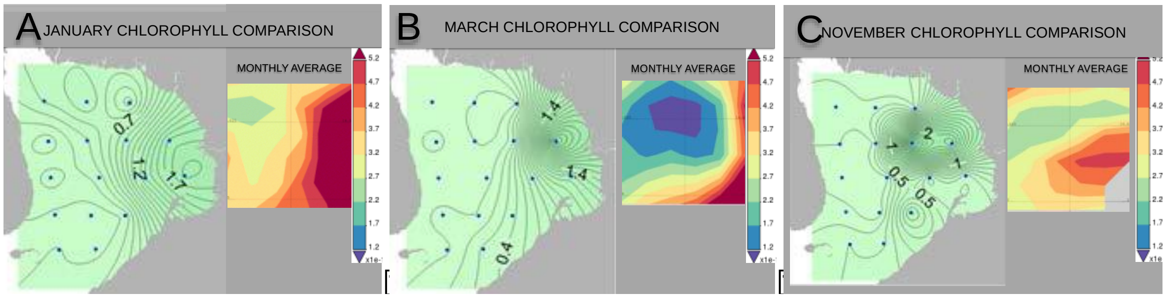


**Figure 5: *In situ* chlorophyll measurements taken in 2013 are compared with patchiness that was identified with Giovanni monthly averaged normalized fluorescence line height (NFLH). Chlorophyll data are extracted from Jose et al. (2015).**

## RESULTS AND DISCUSSION

*Spectral signature and temperature maps*

Remote sensing reflectance can be diagnostic if appropriate selection of wavenelengths is considered in the spectral region where substances either absorb or reflect. As shown in Figure 6,

reflectance at 0.667mµ and 0.678µm gives a correlation coefficient of 0.992. Considering the absorption of chlorophyll at 0.667µm and the increasing reflectance at 0.678 µm (refer to Figure 4A), the high correlation indicates that reflectance at both wavelengths is a result of other substances but chlorophyll, and that both bandwidth carry similar information. In Figure 6, a similar conclusion is derived from the comparison of Rrs reflectance at 0,667µm and 0.555 µm, while the scatter diagram for NFLH at 0.678µm shows a wider dispersion of the data. The comparison of data at wavelengths 0.667µm and 0.443µm shows low reflectance and clustering of data that is charcteristic for coastal waters. The low correlation of 0.606 µm indicates that the two channels respond separately to different components in the water column.

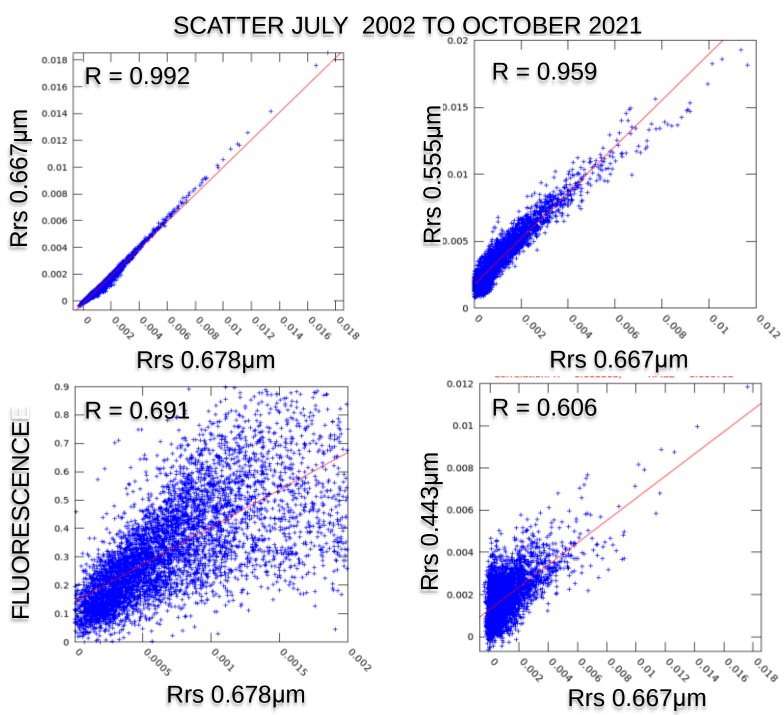


**Figure 6: Scatter diagrams for relating spectral response of bay water and fluorescence. Units of remote sensing reflectance are in $R_{rs}$) $sr^{-1}$, and for (NFLH), in mW $cm^{-2}$ $\mu m^{-1}$ $sr^{-1}$.**

Maps of spectral parameters of Manila Bay are shown in Figure 7. General bio-physical characteristics of Manila Bay are shown with the NFLH, sea surface temperature (SST) and the selected spectral bands. Despite the intense changes that take place from one monsoon season to another, the average maps delineate the various environmental regimes in the bays ecosystems. The distribution of NFLH shows the longitudal east-west gradient as a result of the Pasig River that has a large contribution to eutrophication in the bay, as is shown with the highest values found at the eastern part of the bay along a south-north orientation. The corresponding temperature map in Figure 7B shows lowest temperatures towards the entrance of the bay with a bending of the thermal gradients towards the northwest. The temperature difference between the entrance and the northwest part of the bay is about one centigrade but the distribution of NFLH and SST are not correlated.

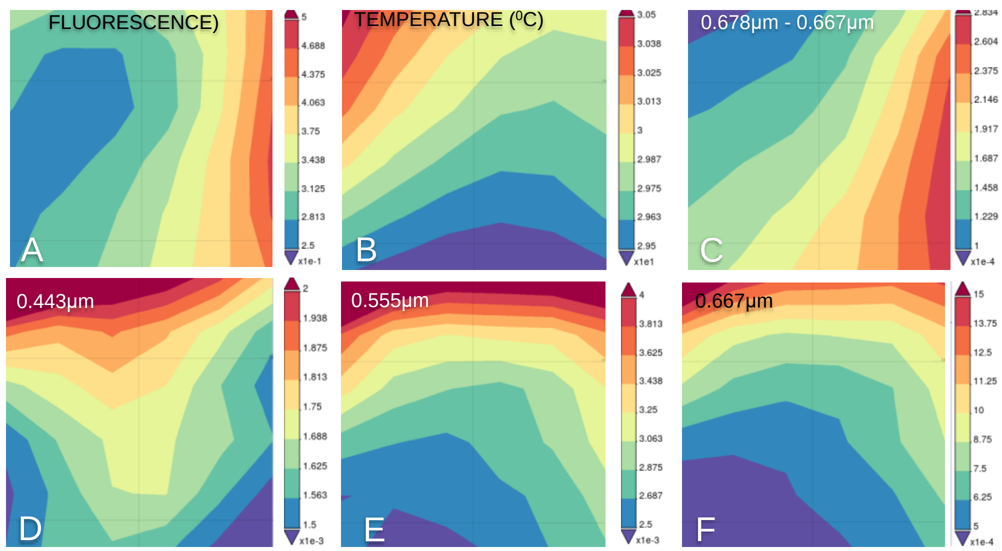


**Figure 7: Spectral interpretation of water parameters in Manila Bay with time averaged maps from 2002 to 2021. A: Fluorescence in mW cm$^{-2}$ µm$^{-1}$ sr$^{-1}$. B: Sea surface temperature ($^{0}$C). Figures C to Figure F are given as remote sensing reflectance where Figure C is the spectral difference of remote sensing reflectance between 0.678µm and 0.667µm; D: reflectance at 0,443µm over the first chlorophyll absorption band; E: reflectance at 0.555µm that is diagnostic for particulate; F: reflectance is located at 0.667µm over the second asorption band of chlorophyll.**

Figure 7C shows the difference between the two wavelengths that are related to the second chlorophyll absorption band at 0.667µm and 0.678µm that is related to fluorescence of chlorophyll in living phytoplankton organisms. The difference-map shows a similar distribution pattern as the fluorescence data with lowest values observed in the northwest of the bay and maximum values observed in the western part of the test site that is under the influence of outrunning water from the Pasig River. Figure 7D shows the map for the spectral region at 0.443µm in which the α-absorption band of chlorophyll is located. However, chromophobic dissolved organic matter (CDOM) also absorbs strongly at this wavelength, and high turbidity of river water adds to reflectance values. Therefore, the response at this wavelength is a result of several constituents in the water especially those that are derived from the river effluent. This is indicated by the reflectance values in the nearshore region compared to those towards the bay entrance. Figure 7E shows the reflectance map for the wavelength at 0.555µm. This spectral region shows less the influence of specific absorption bands but provides information on supsended matter either in inorganic or organic form because even living algal cells contribute at this wavelength a signal that originates from scattering at their outer shell. The distribution of reflectance data at wavelength 0.667µm shows a similar pattern to data based on values at 0.555µm. Although the data have a different amplitude, they demonstrate that the reflectance at the position of the second absorption band , is also impacted by scattering of particles.

The NFLH is substance specific and is not necessarily correlated with substances that have spectral signatures at various wavelengths as is shown in Figure 8 with NFLH and remote sensing reflectence at different wavelenghts. In general, the coefficients are low. Temperature seems to be a minor factor in controlling phytoplankton abundance in the bay although sea surface temperature changes in the bay adds occasionally to vertical density stratification. Correlation of fluorescence and $R_{rs}$ at 0.443µm ranges from 0.2 in the north to -0.2 in the south of the bay; at 0.531µm, the coefficient shows only positive values while the best correlation is found at 0.678µm.

The image at 0.667µm shows relatively high correlation with NFLH that is antcicipated at wavelengths 0.667µm and at 0.678µm. Moreover, the correlation of the image at 0.678µm and the NFLH provides evidence that the surface signature in the southern part of the site is more related to chlorophyll.

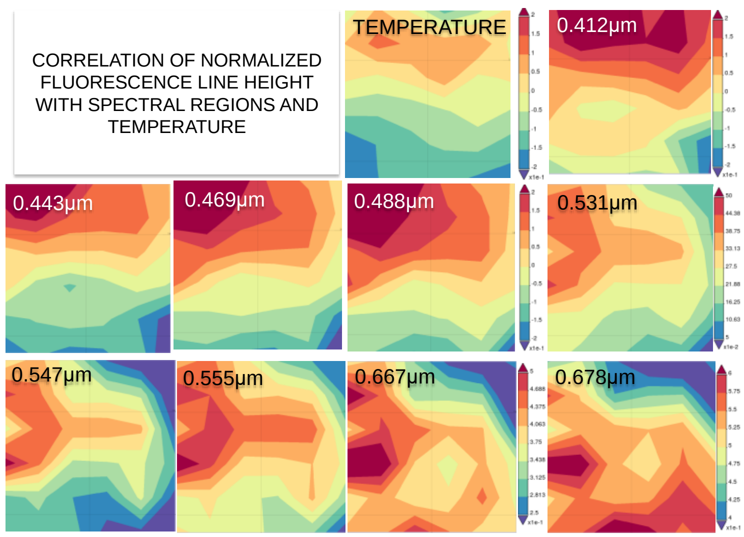


**Figure 8: Correlation of normalized fluorescence line height with sea surface temperature and different wavelenghts of bay water (refer to Figure 5). The color annotations for the images are indicated on the right.**

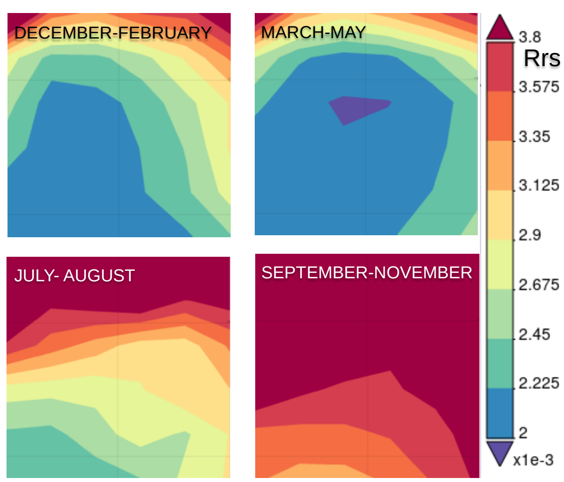


**Figure 9: Seasonal average of Rrs at 0.555µm by seasons covering March 2002 to June 2021.**

*Averaged seasonal maps*

The environmental changes in Manila Bay are recognized with seasonal maps for NFLH, $R_{rs}$ at 0.555µm and surface temperature. The distribution of $R_{rs}$ at 0.555µm in Figure 9 shows the lowest values from December to May and high values from September to November indicate the influence of river discharge. Similar changes are also shown with NFLH in Figure 10.

NFLH shows the lowest fluorescence during March to May when river discharge is low and wind direction dominates from the southeast. The other seasons show high values in the eastern part of the site but during the southwest monsoon from September to November, the bay shows maximum values.

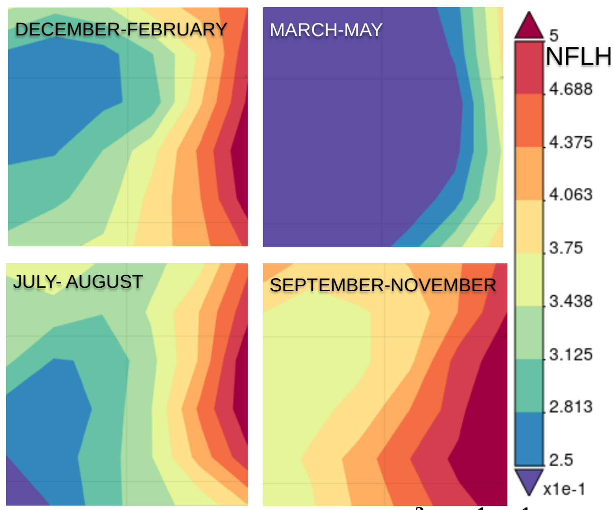


**Figure 10: Seasonal average maps of NFLH in mW cm$^{-2}$ µm$^{-1}$ sr$^{-1}$ covering March 2002 to June 2021.**

The distribution pattern recognized with NFLH and $R_{rs}$ at 0.555µm is not realized in the sea surface temperature distribution. Rather a south-north gradient of temperature is documented in Figure 11 with the lower temperature indicating the influence of cooler costal water, whereas the northeastern part adjacent to the coast has the highest temperature during all seasons.

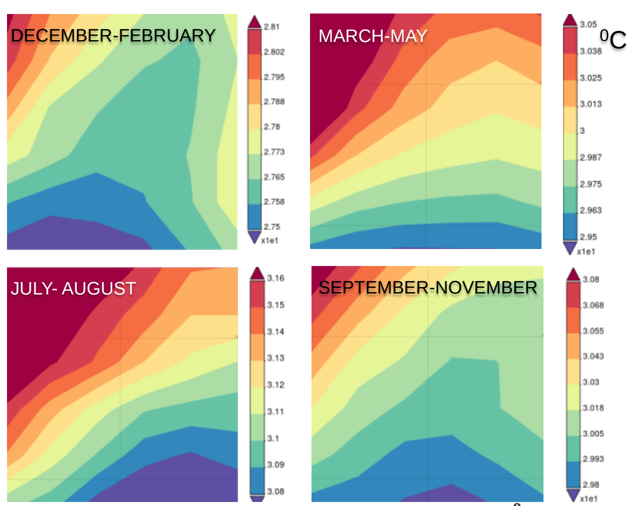


**Figure 11: Seasonal average maps of sea surface temperature ($^{0}$C) covering March 2002 to June 2021. Note that for each season, a different range of color annotations has been applied in order to account for the seaonal range in temperature changes.**

*Monthly maps averaged from 2002 to 2021*

Yearly averaged data mask changes and more details in the distribution patterns of NFLH that are shown in Figure 12 with monthly averaged data in relation to the wind direction. The maps for February to May show the lowest NFLH coinciding with reduced river discharge of the Pampanga and Pasig Rivers that have their minimum discharge in March/April and in May, respectively (Siringan and Ringor, 1998). During the southwest monsoon season, from June to September, the fluorescence is comparably low. The season during which the Pasig and Pampanga Rivers start to increase their discharge corresponds with the increasing NFLH values in August in the eastern part of the bay. Before the onset of the northeast monsoon, the interim period in October has also elevated NFLH but the values increase further from November to December. At the end of the northeast monsoon, the NFLH starts to decline again as seen with the January map.

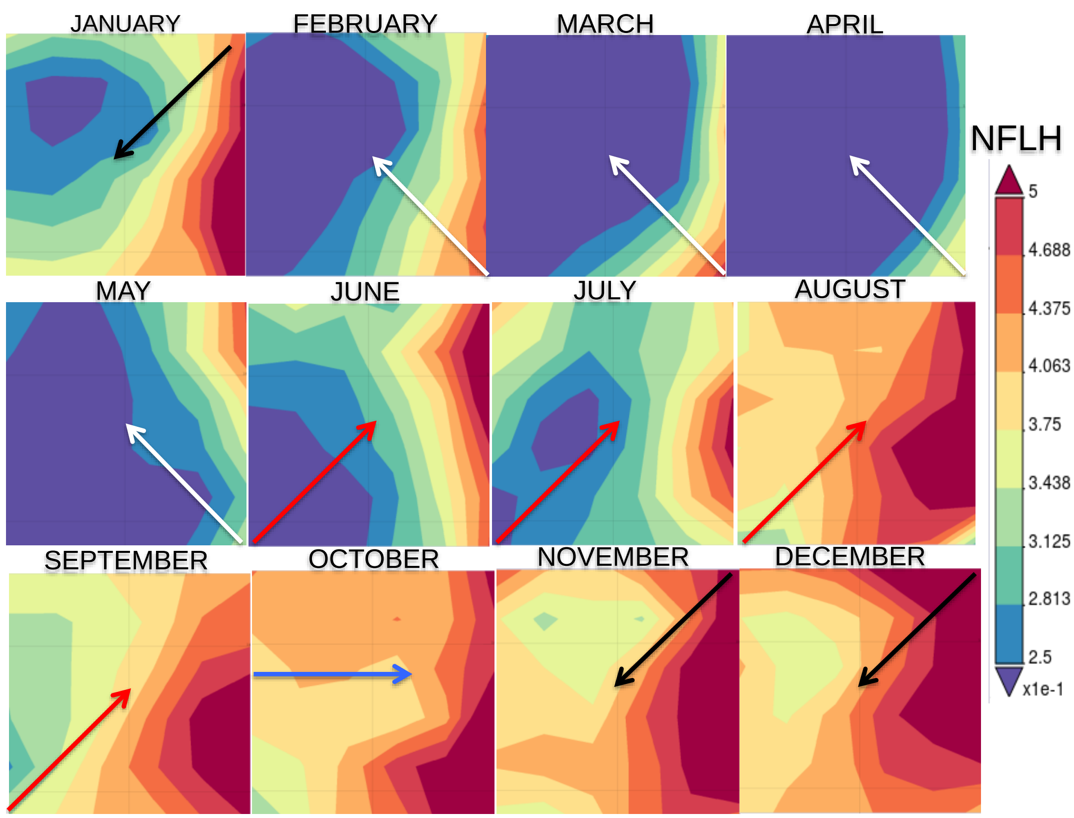


**Figure 12: Monthly fluorescence line height (FLH) in mW cm$^{-2}$ µm$^{-1}$ sr$^{-1}$ averaged from 2002 to 2021. Arrows indicate the average major wind direction (refer to Figure 2).**

*Selected single monthly images for 2002 to 2021*

With NFLH data that are averaged over almost two decades, anomalies that are related to changes within the yearly cycle may go unnoticed. In order to recognize monthly changes, data were selected that had complete monthly coverage of the test site and were grouped in chronological order and are shown in Figures 13 to 16. The season from February to May yields the highest number of images with a full coverage of the bay, and the selected images are shown in Figure 13. The images were taken during the season when the southeast winds are dominant and lower cloud frequency provided occasionally complete coverage of the bay within one month. The surface currents during this season are mainly cyclonic (Villanoy and Martin, 1997) and the highest values for NFLH are found in the eastern and

***Research Article***

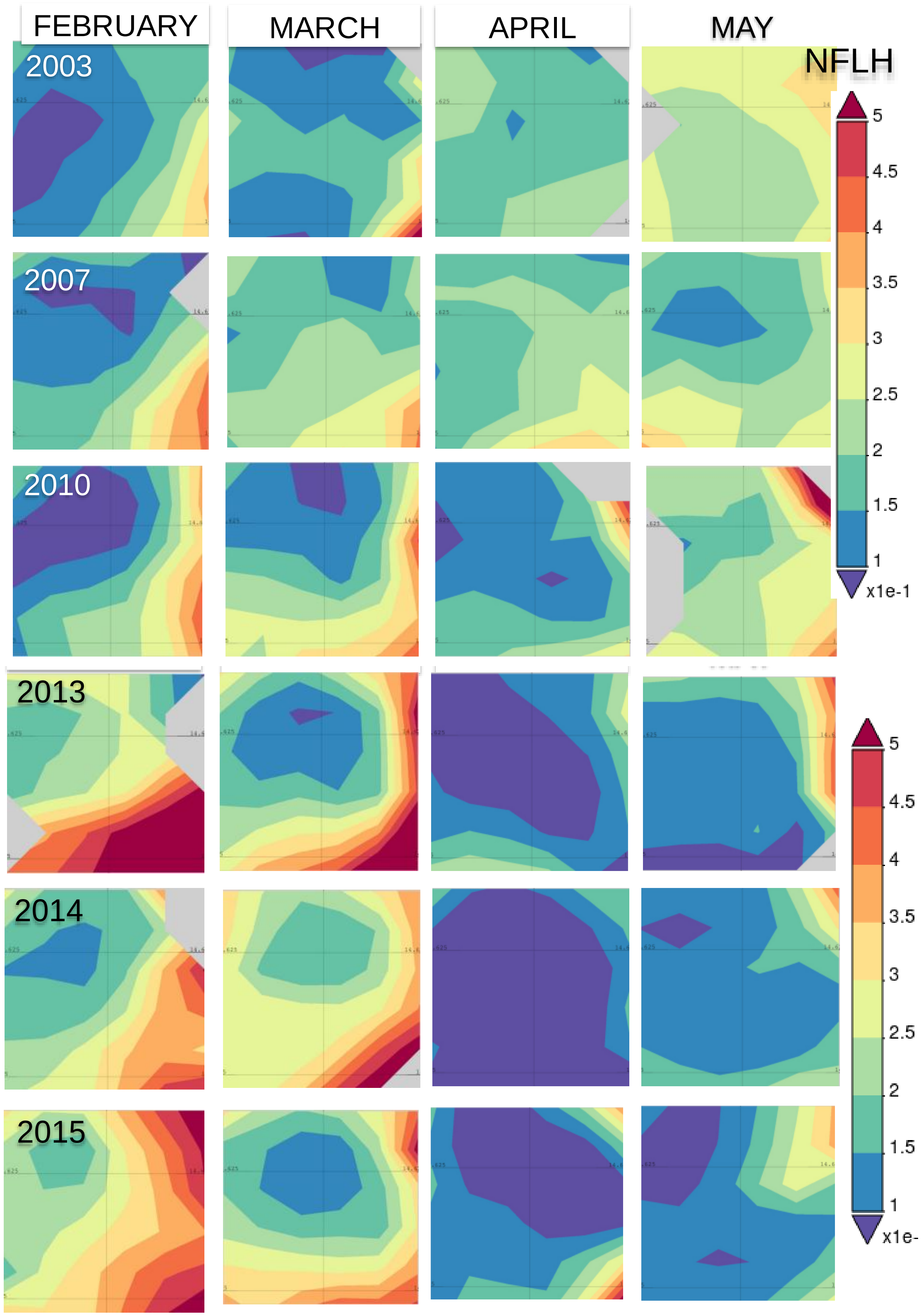


**Figure 13: Selected monthly averaged images of NFLH with full-coverage February to May 2002 to 2021.**

***Research Article***

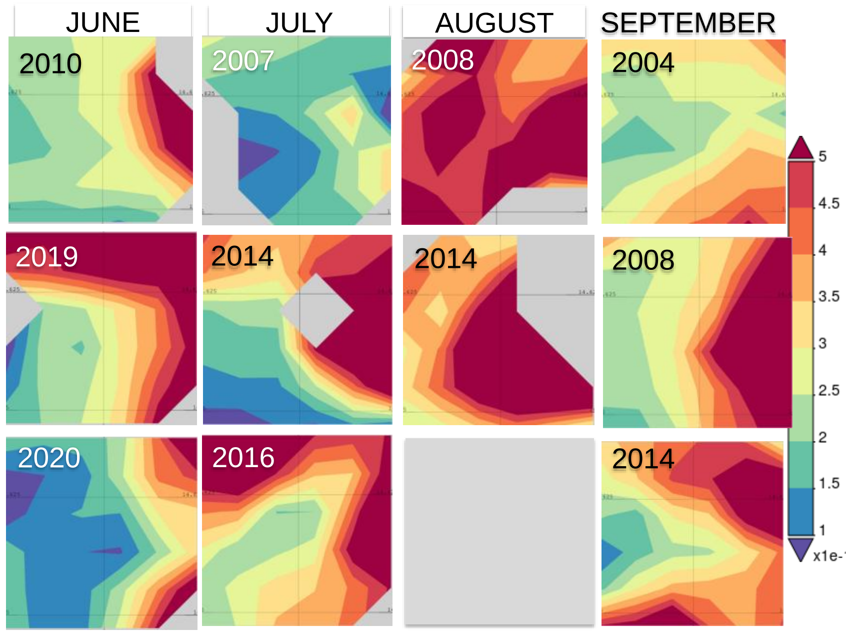


**Figure 14: Selected monthly averaged images of NFLH with full-coverage for June to September 2002 to 2021.**

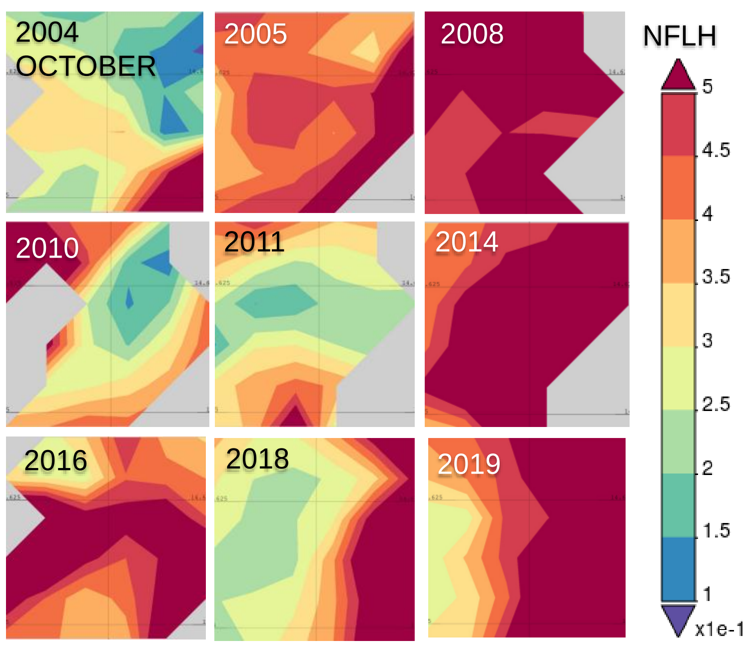


**Figure 15: Selected monthly averaged images of NFLH with full-coverage for October 2002 to 2021.**

southern parts during February. In March, the center of the bay has decreasing values, and minimum values are located in the center of the cyclonic water movement. This circular arrangement of minimum

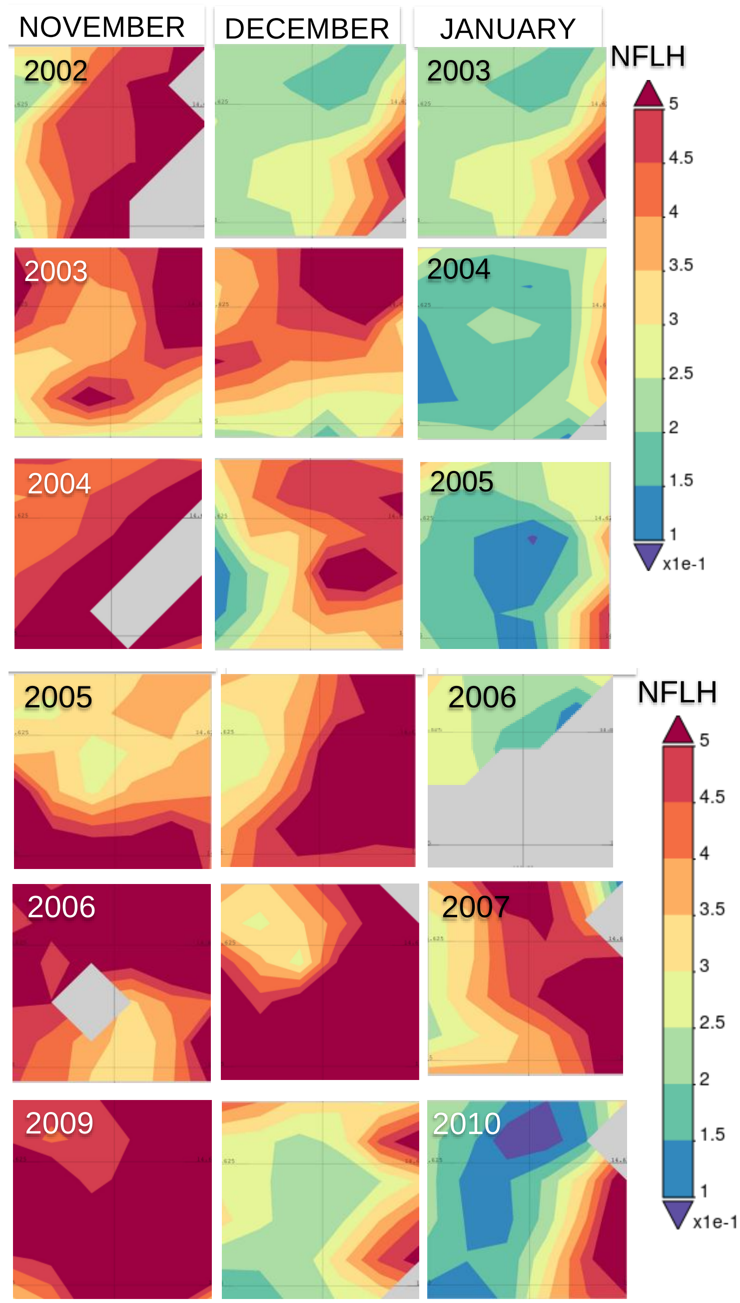


**Figure 16: Selected monthly averaged images of NFLH with full-coverage for November to January 2002 to 2021.**

NFLH has been recognized every year in images even when the test site was not completely covered. Decrease of NFLH continues until April when the site showed minimum fluorescence. Towards May, an increase of NFLH is observed at the eastern part of the bay when the transition time from southeasterly winds to southwesterly winds emerges.

Figure 14 shows selected images that cover the period June to September when the southwesterly winds drive the surface currents in an anticyclonic movement and when there is increasing discharge from the Pampanga and Pasig Rivers. In August, due to the dense cloud cover, only two images for 2008 and 2014 were useful but they show that the bay had an increasing NFLH and that high heterogeneity is observed.
October is considered as the interim period for the change from the southwest to the northeast monsoon. Due to high frequency of cloud coverage in October, only a few useful images over a time frame of twenty years were obtained and are shown in Figure 15, and demonstrate that during the transition from southwesterly to northeasterly winds, large fluctuations in NFLH values can be found especially along the eastern part of the observation site. During the northeasterly winds, the bay shows high NHFL in the November coverage but in December and January, lower values are observed. This change concurs with the lessening of river discharge from the two freshwater contributors to the bay
The appearance of the minimum in the center of the test site is a persistent and characteristic feature of the bay that is also recognized with zonal longitudal NFLH means that are compared with corresponding temperatures in Figure 17. While the temperature shows gradual increase from south to north, the NFLH goes through a minimum at the center.

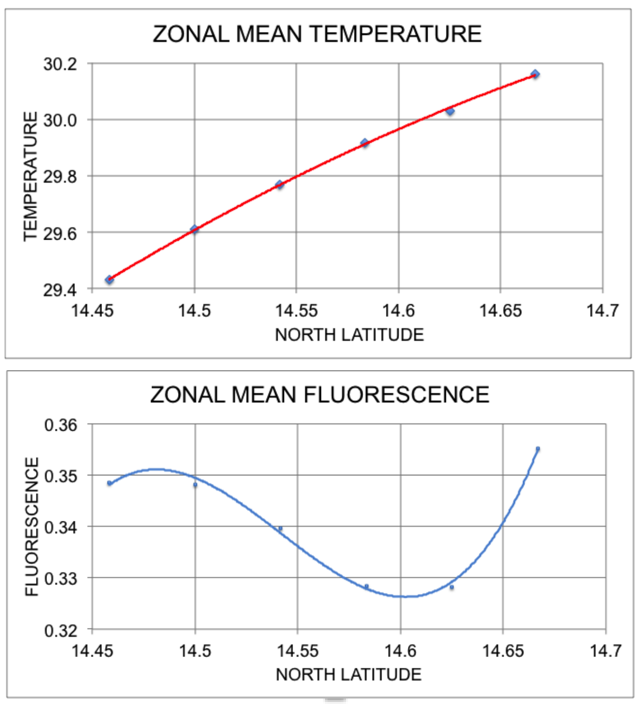


**Figure 17: Manila Bay zonal mean of longitude for sea surface temperature and NFLH based on data averaged from July 2002 to November 2011. Both data sets have been subjected to 3$^{rd}$ order polynomial fits .**

*Temporal changes*
Temporal resolution of data shows complexity that appears in different patterns especially those that are related to monsoonal changes. In addition to spatial and temporarial heterogeneity, there is also spectral heterogeneity introduced by changes in species composition and varying contributions of dissolved and particulate matter either in organic or inorganic form. Thus the pattern recognized in the distribution of NFLH is caused by various and sometimes independent processes. In Figure 18 a higher temporal resolution is used for the test site with a time sequence of monthly longitude-averaged data, covering the

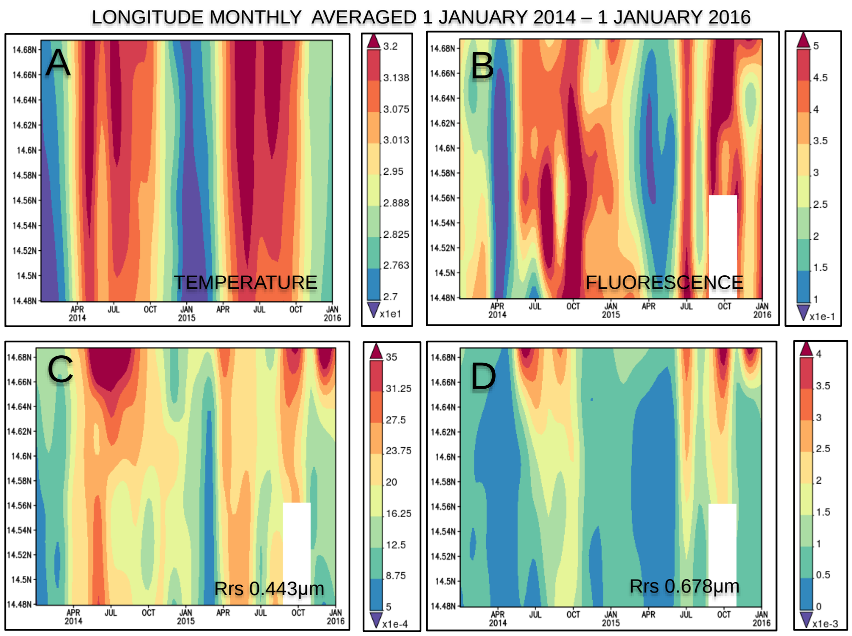


**Figure 18: Hovmöller longitude-averaged data from January 2014 to January 2016. A: Sea surface temperature; B: NFLH; C: $R_{rs}$ at 0.443 µm; D: $R_{rs}$ at 0.678µm.**

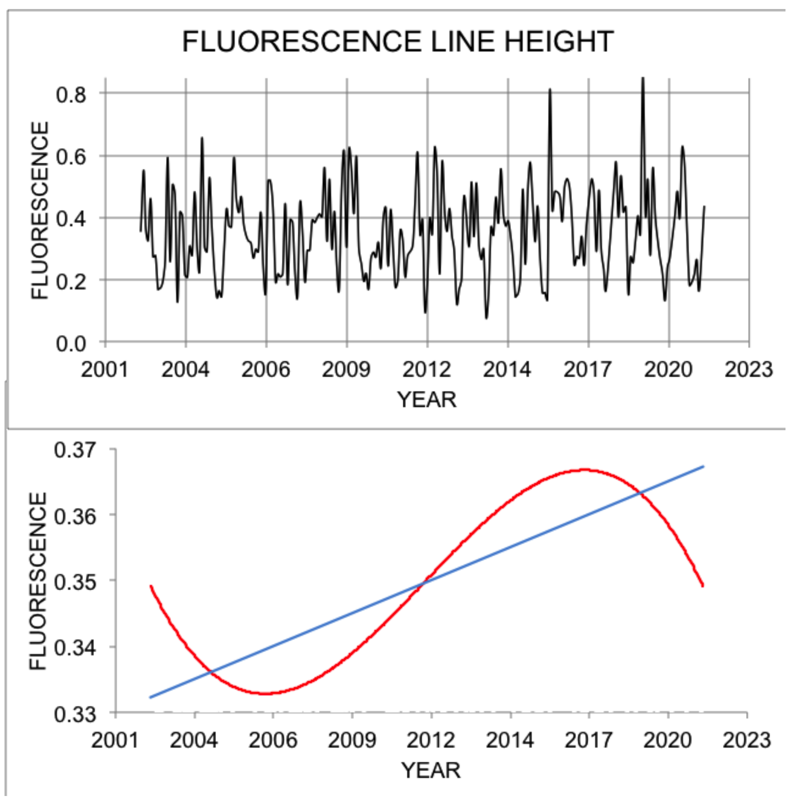


**Figure 19: Time series of monthly-averaged NFLH in area site of Manila Bay. The blue line gives the linear regression and the red line shows the 3rd order polynomial fit.**

period January 2014 to January 2016, and are shown for temperature and NFLH $R_{rs}$ 0.443µm and $R_{rs}$ 0.678µm. The images show that temperature in the central part of the bay undergoes the typical cycling in response to the monsoonal changes but display a rather smooth transition from one season to another. Only during the southwest monsoon, can significant temperature changes be rcognized. The NFLH image shows that most of the elevated fluorscence is related to the southwest monsoon although higher values continue to occur during the northeast monsoon. Contrary to the temperature distribution, the NFLH shows high patchinesss and gradients that are not always aligned with temperature gradients. Similarly, the $R_{rs}$ at 0.443µm and 0.678µm show patchiness that is not always aligned with temperature gradients, and distribution patterns that deviate from those of NFLH are mostly visible in the northern part of the bay.

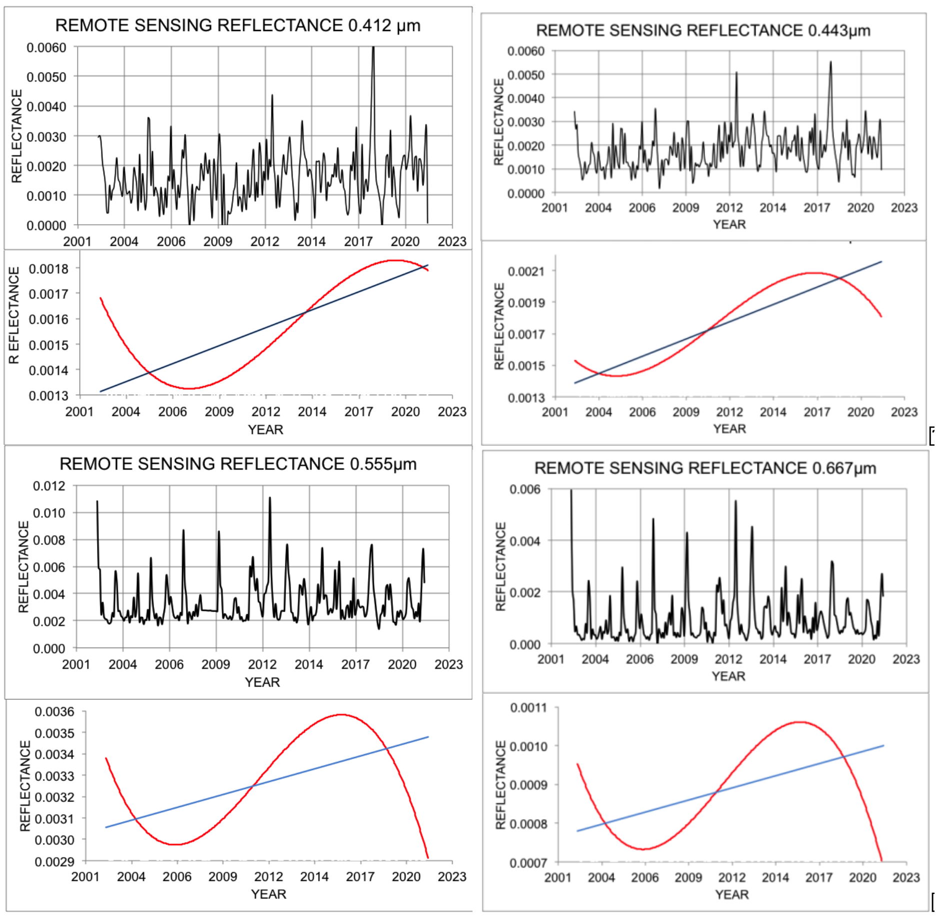


**Figure 20: Time series of monthly-averaged spectral regions at 0.412µm, 0.443µm, 0.555m and 0.667µm. The blue lines present linear regressions and the red lines show 3rd order polynomial fits.**

The time series of monthly-averaged NFLH in Figure 19 follows the monsoonal changes with minima observed during the time of southeasterly winds and low river discharge, and maxima are found during the southwest monsoon. Although monthly averaged data suppress partly the detection of short-lived blooms, they can still be recognized in monthly averaged data through the appearance of sudden peaks in NFLH. However, blooms of green and red *Noctiluca* have been observed in Manila Bay on July 2012 and January 2014 (Borja *et al.*, 2019) but are not recognized in monthly-averaged NFLH data. That shows that the 4-km resolution of data does not recognize small scale blooming especially when it occurs at a short time scale and is restricted to small coastal areas. Patchiness in the distribution of fluorescence is generally concentrated on the eastern part of the bay. This is also in agreement with measured chlorophyll concentrations throughout 2014 and at the end of 2015 that showed high concentrations in the eastern and southwestern part of the bay (Poniente and Santos, 2017), and that blooming can be attributed mainly to river discharge (Poquita-du and Todd, 2015).

Changes observed with NFLH are also recognized in remote sensing reflectance at various wavelengths that are shown in Figure 20. Linear regressions and polynomial fits show changes that are close to the time frame of global change events, and values increased at all wavelengths of $R_{rs}$. Based on linear regression, the highest increase is found in the blue region at 0.412µm and 0.443µm of around 30%. At $R_{rs}$ 0.667µm, close to the second absorption band of chlorophyll, the increase is about 20%. $R_{rs}$ at 0.555µm, and the NFLH yield an estimated increase of about 10%.

Although not necessarily linearly correlated, the changes at various wavelengths indicate that the observed increase in reflectance and fluorescence is a result of additional biomass. A rough estimate for chlorophyll changes can be made with fluorescence measurements and ship-borne chlorophyll measurements (chlorophyll = 4.726x - 0.299, where x=fluorescence in NFLH units). Accordingly, the bay has an average concentration for 2002 of 1.27mg $m^{-3}$, and for 2022, it has 1.44mg $m^{-3}$, that corresponds to a change of approximatly 0.009 mg $y^{-1}$. It has to be emphasized that these estimates are approximations based on an average over twenty years that smooths out the large seasonal changes. This is documented in Figure 21 where the slopes of interannual NFLH show significant fluctuations from one season to another, and high variation occurs even within each season. Furthermore, the direction of the trend changes. For December to February and September to November, a positive change is observed while the season March to May shows a negative trend, and the smallest increase is recognized for June to August when southeasterly winds prevail.

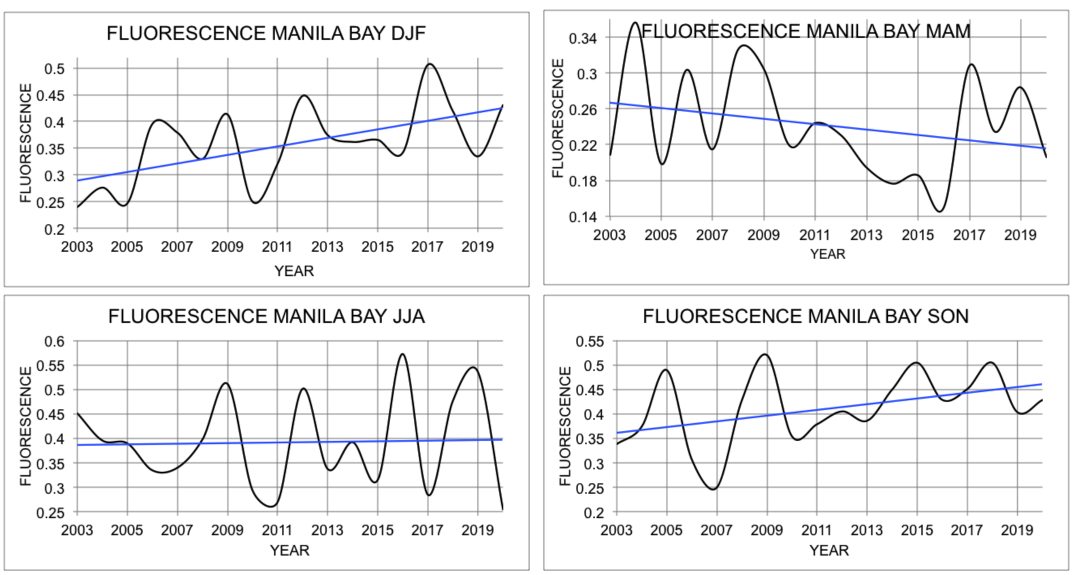


**Figure 21: Area averaged interannual NFLH for December to February (DJF); March to May (MAM); June to August (JJA) and September to November (SON). The blue lines indicate linear regressions.**

*Temperature fluctuations in Manila Bay*

The temperature series in Figure 22 shows seasonal changes with maxima at the end of the year although short fluctuations before cooling starts during the northeast monsooon. Figure 22A shows the temperaure

***Research Article***

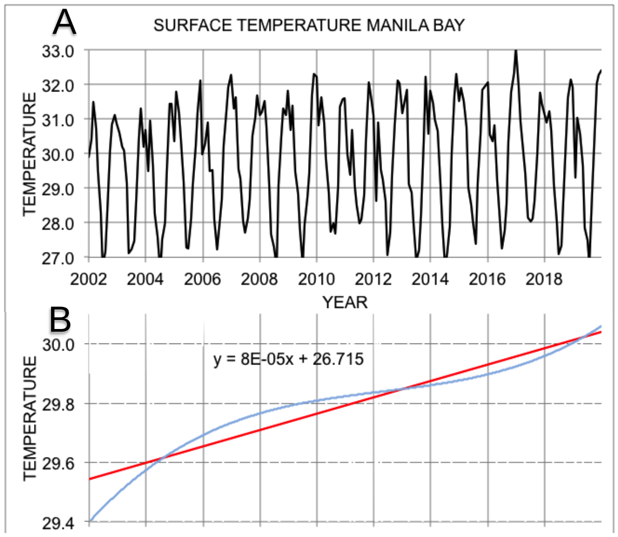


**Figure 22: A: Area averaged monthly temperature series in Manila Bay: B. Expanded scale from A with linear regression in red and 3rd order polynomial fit in blue.**

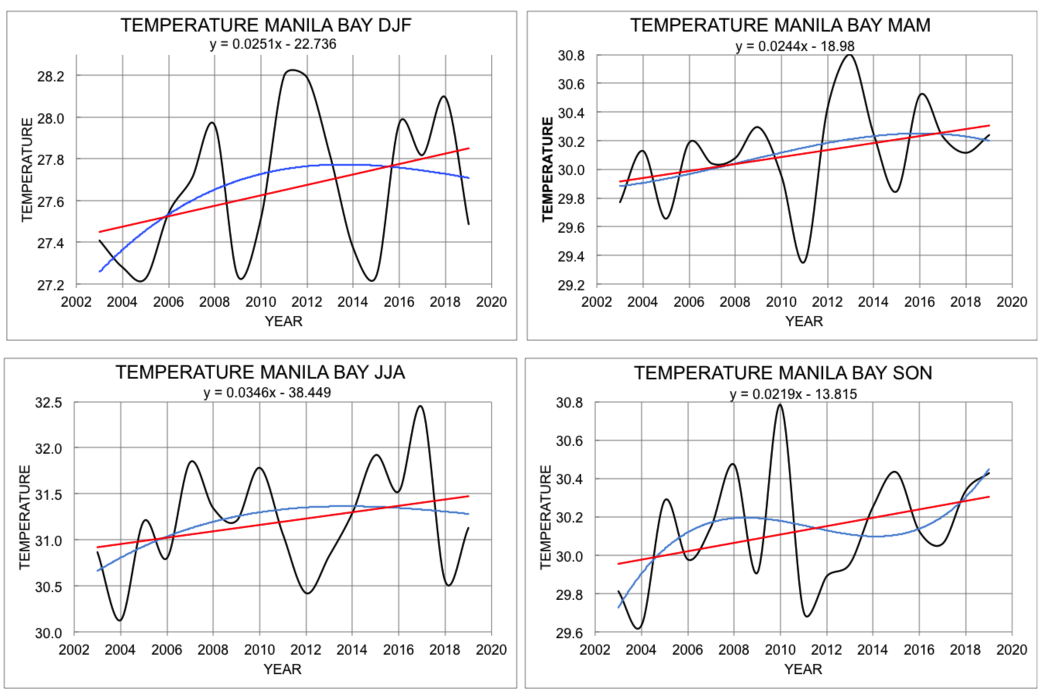


**Figure 23: Area averaged interannual sea surface temperature changes in Manila Bay. Linear regressions are shown in red and 3rd order polynomial fits are shown in blue.**

distribution that ranges between $27^0$ C and $33^0$ C. Linear regression and 3rd order polynomial fit as shown in Figure 22B reveal a temperature increase of about 0.028 C $y^{-1}$. This temperature increase of Manila Bay is similar to the range of sea surface temperature around the Philippine coastal water that was estimated with monthly-averaged sea surface temperature series indicating that the Philippines follows the global trend in ocean temperature increase (Szekielda and Guzman (2021).

Subdividing the data into seasons, as is shown in Figure 23, reveals a more detailed picture of the observed temperature increase. The interannual differences show for all seasons with linear regressions a common trend towards higher temperatures. Due to the high variations in the interannual data, the use of the 3rd order polynomial fit is not conclusive although the corresponding trend shows a slight adjustment of temperature towards lower values.

Slope changes in temperature and NFLH are symptomatic for each season and therefore grouping of data by months allows the isolation of the months during which anomalies may be anticipated. Table 1 summarizes linear regressions that were used to estimate the monthly temperature for 2000 and forecast the possible temperature for 2035. Furthermore, an estimate of yearly rate-change was derived from the temperature difference of 2000 and 2035. The NFLH data have been equally processed and the temperatures and results are listed in Table 2.

**Table 1: Estimated monthly sea surface temperature in Manila Bay based on linear regression of data from January 2002 to December 2020 and estimated rate change that were used to forecast the possible temperature for 2035.**

.

| MONTH | EQUATION | 2000 | 2035 | $^{0}C\ y^{-1}$ |
|---|---|---|---|---|
| **JANUARY** | y = 0.0411x - 55.37 | 26.84 | 28.28 | 0.041 |
| **FEBRUARY** | y = 0.0078x + 12.04 | 27.64 | 27.91 | 0.008 |
| **MARCH** | y = -0.0027x + 34.02 | 28.62 | 28.53 | -0.003 |
| **APRIL** | y = 0.0111x + 7.93 | 30.13 | 30.52 | 0.011 |
| **MAY** | y = 0.0633x - 95.63 | 30.97 | 33.19 | 0.063 |
| **JUNE** | y = 0.0485x - 65.91 | 31.09 | 32.89 | 0.051 |
| **JULY** | y = 0.0494x - 67.98 | 30.82 | 32.55 | 0.049 |
| **AUGUST** | y = 0.0318x - 33.19 | 30.41 | 31.52 | 0.032 |
| **SEPTEMBER** | y = 0.0079x + 15.08 | 30.87 | 31.15 | 0.008 |
| **OCTOBER** | y = 0.0529x – 76.24 | 29.56 | 31.41 | 0.053 |
| **NOVEMBER** | y = 0.0136x + 1.79 | 28.99 | 29.47 | 0.014 |
| **DECEMBER** | y = 0.0573x - 87.23 | 27.37 | 29.38 | 0.057 |

**Table 2: Estimated monthly NFLH ($FLy^{-1}$) in Manila Bay based on linear regression of data from January 2002 to December 2020 and estimated rate change.**

| MONTH | EQUATION | 2000 | 2035 | $FLy^{-1}$ |
|---|---|---|---|---|
| **JANUARY** | y = 0.0090x - 17.780 | 0.220 | 0.535 | 0.0090 |
| **FEBRUARY** | y = 0.0098x - 19.520 | 0.081 | 0.424 | 0.0098 |
| **MARCH** | y = 0.0035x - 6.705 | 0.295 | 0.418 | 0.0035 |
| **APRIL** | y = -0.0017x + 3.680 | 0.280 | 0.221 | -0.0017 |
| **MAY** | y = -0.0107x +21.882 | 0.482 | 0.108 | -0.0107 |
| **JUNE** | y = -0.0055x +11.473 | 0.473 | 0.281 | -0.0055 |
| **JULY** | y = 0.0064x - 12.463 | 0.337 | 0.561 | -0.0064 |
| **AUGUST** | y = -0.0007x + 1.809 | 0.409 | 0.385 | -0.0007 |
| **SEPTEMBER** | y = 0.0023x - 4.194 | 0.406 | 0.487 | 0.0023 |
| **OCTOBER** | y = 0.0160x - 31.761 | 0.239 | 0.799 | 0.0160 |
| **NOVEMBER** | y = -0.0007x + 1.752 | 0.352 | 0.328 | 0.0007 |
| **DECEMBER** | y = 0.0056x -10.907 | 0.293 | 0.489 | 0.0056 |

If the trend persists, the temperature estimates in Figure 24 show that increase in warming by 2035 will be mainly during the period of southwest winds when the surface circulation of the bay is in anticyclonic mode whereas minimal warming can be foreseen especially during the months of southeast winds when cyclonic movement in the bay persists.

***Research Article***

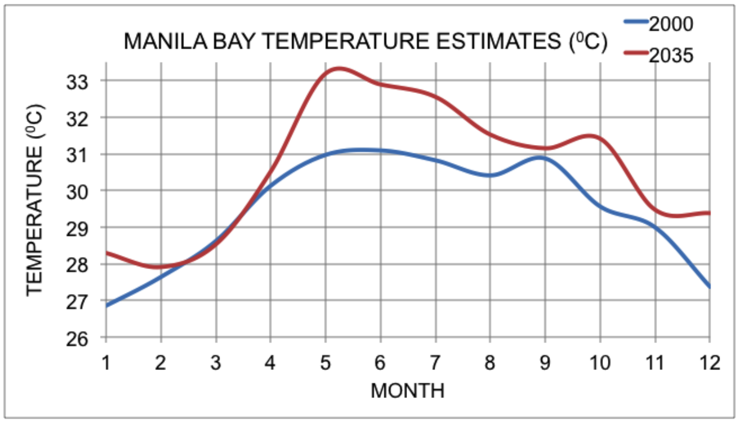


**Figure 24: Temperature estimates for 2000 and 2035 based on linear regression of data from January 2002 to December 2020 as shown in Table 1.**

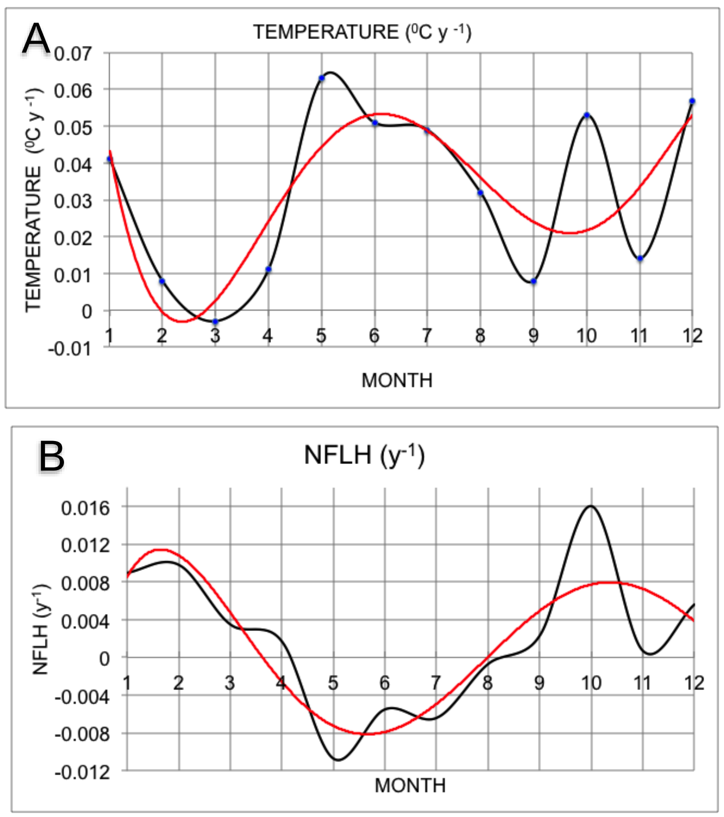


**Figure 25: Change in rate ($y^{-1}$) based on linear regression of data from January 2002 to December 2020. A: Estimated average temperature rate change between 2000 and 2035 as listed in Table 1. B: Estimated average NFLH rate change between 2000 and 2035 as listed in Table 2. The red lines show polynomial fits.**

The calculated rates of changes between 2000 and 2035 for temperature and NFLH are shown in Figures 25A and B. The rate of temperature increase shows minimum warming for March, highest for May/June, and two additional minima are observed for September and November, respectively. The polynomial fit shows that seasonal aspects have to be considered when discussing the anticipated increase in temperature and its possible impact on environmental conditions. Temperature and NFLH have opposite trends and the minimum of NFLH falls together with the maximum increase of temperature during the southwest monsoon, while increased NFLH coincides with decreasing temperature during February/March and around October. The observed negative rate change of NFLH during the southwest monsoon does not necessarily indicate a reduction in biomass, rather a redistribution of dense plankkton blooms at the surface, and increased turbulance can also be assumed as a cause for the declining values. However, any forecasting of parameters that are related to the marine ecosystem have to be evaluated with caution because they develop on a different spatio-temporal scale compared to temperature changes.

## FINAL REMARKS

The use of fluorescence (NFLH) as an indicator for biomass and the use of reflectance at different wavelengths provide insight into changes at different time scales. The observed temperature increase is especially significant for all seasons, and increasing fluorescence data show that eutrophication of the bay still continues. However, correlations indicate that temperature is not the primary driver in increasing NFLH, rather a secondary effect such as change in vertical turbulence and density stratification of the bay and most importantly, increasing nutrient flux, may be reasons for blooming effects as is indicated by seasonal differences in slope of NFLH and sea surface temperature. Furthermore, the distribution pattern of the various parameters and their intensity seem to be more linked to seasonal and large-scale changes of the monsoon seasons and changes of the surface circulation in the bay. In addition, the emission of anthropogenic material into the bay is most probably the prime driver in changes of the ecosystem in the bay.

The linear regressions used in this study provide the general trend of external forcing from anthropogenic gases and aerosols, whereas the long-term trend expressed by polynomial fits seem to follow more internal decadal variations. Global changes are well reflected in analyzed temperature and NFLH, and could be related to the Inter-decadal Pacific Oscillation that dominates decadal variations in global mean surface temperature (Dong and McPhaden, 2017). Furthermore, global mean surface temperature shows considerable pronounced warming trend for 2001–2013 and accelerated warming appears to be underway, with record highs in global temperature in 2014, 2015, and 2016. The comprehensive survey of Manila Bay with data that span over almost two decades allowed to follow the development of those changes that are related to climatic changes in global events and illustrates that the Philippine marine environment is not an exemption in following global climate trends

## ACKNOWLEDGEMENTS

The author is affiliated with Columbia University EEC as Research Associate and with the Ateneo University de Manila Department of Environmental Science (DES) as Fulbright Alumnus and International Faculty Member. He is grateful for the opportunity to be sponsored through DES. Analyses and visualizations used in this study were produced with the Giovanni online data system, developed and maintained by the NASA GES DISC. The MODIS mission scientists and associated NASA personnel are acknowledged for the production of the data used in this research effort.

## REFERENCES

**Acker JG and Leptoukh G (2007)**. Online Analysis Enhances Use of NASA Earth Science Data, *Eos Trans. AGU* **88** (2) 14-17.

**Behrenfeld MJ, O'Malley RT, Siegel DA et al. (2006)**. Climate-driven trends in contemporary ocean productivity. *Nature*, **444** (7120). 752-755. doi:10.1038/nature05317.

**Behrenfeld MJ, Westberry TK, Boss ES, O'Malley RT, Siegel DA, Wiggert JD, Franz BA, McClain CR, Feldman GC, Doney SC, Moore JK, Dall'Olmo G, Milligan AJ, Lima I, and Mahowald N**

**(2009)**. Satellite-detected fluorescence reveals global physiology of ocean phytoplankton. *Biogeosciences* **6** 779–794. www.biogeosciences.net/6/779/2009/.

**Borja VM, Furio EF, Gatdulal N, Iwataki CM (2019)**. Occurrence of harmful algal blooms caused by various phytoplankton species in the last three decades in Manila Bay, Philippines. *Philippine Journal of Natural Sciences* **24** 80-90.

**Boyce DG, Lewis, MR and Worm B (2010)**. Global phytoplankton decline over the past century. *Nature,* **466** (7306) 591–596.

**Chang KH, Amano A, Miller TW, Isobe T, Maneja R, Siringan FP, Imai H, and Nakano S (2009)**. Pollution Study in Manila Bay: Eutrophication and Its Impact on Plankton Community. *Interdisciplinary Studies on Environmental Chemistry - Environmental Research in Asia* 261-267.

**Clemente ED (2020)**. Evaluating the water quality contribution of Estero de Paco to Pasig River and Manila Bay, Philippines. E3S Web of Conferences 148, 07010. https://doi.org/10.1051/e3sconf/202014807010.

**De Las Alas JG and Sodusta JA (1985).** A model for the wind driven circulation of Manila Bay, *National Applied Science Bulletin* **37** (2) 159-170.

**Dong L and McPhaden MJ (2017).** The role of external forcing and internal variability in regulating global mean surface temperatures on decadal timescales. *Environ. Res. Lett. 1-10.***12** 034011.

**Gorme JB, Maniquiz MC, Song P, Kim L-H (2010)**. The Water Quality of the Pasig River in the City of Manila, Philippines: Current Status, Management and Future Recovery. *Environmental Engineering Research* **15** (3) : 173-179. DOI:10.4491/eer. 2010.15. 3. 173. pISSN 1225-1025 eISSN 2005-968X

**Hoegh-Guldberg OD, Taylor JM, Bindi M, Brown S, Camilloni I, Diedhiou A, Djalante R, Ebi KL, Engelbrecht F, Guiot J, Hijioka Y, Mehrotra,S, Payne A, Seneviratne SI, Thomas A, Warren R and Zhou G (2018)** Climate-driven trends in contemporary ocean productivity. In: *Global Warming of 1.5°C. An IPCC Special Report on the impacts of global warming of 1.5°C above pre-industrial levels and related global greenhouse gas emission pathways, in the context of strengthening the global response to the threat of climate change, sustainable development, and efforts to eradicate poverty*, edited by Masson-Delmotte, V. Zhai, A, Pörtner, H-O, Roberts, D, Skea, J, Shukla, PR, Pirani, A, Moufouma-Okia, W, Péan, C, Pidcock, R, Connors, S, Matthews, JBR, Chen, Y, Zhou, X, Gomis, MI, E. Maycock, LT, Tignor, M and Waterfield, T.

**Hu C and Feng L (2016)**. Modified MODIS fluorescence line height data product to improve image interpretation for red tide monitoring in the eastern Gulf of Mexico. *Journal of Applied Remote Sensing* **11**(1), 012003 (2016), doi: 10.1117/1.JRS.11.012003.

**Jacinto GS, Azanza RV, Velasquez IB and Siringan FP (2006a).** Manila Bay: Environmental Challenges and Opportunities. In: *The Environment in Asia Pacific Harbours* edited by Wolanski E. Springer: Dordrecht, Netherlands, 309-328.

**Jacinto GS, Sotto LPA, Senal AIS, McGlone ML, Escobar MTL, Amano A and Miller TW (2011).** Hypoxia in Manila Bay, Philippines during the northeast monsoon. *Marine Pollution Bulletin* **63** 243-248.

**Jacinto GS, Velasquez IB, San Diego-McGlone ML, Villanoy CL and Siringan FB (2006b).** Biophysical Environment of Manila Bay - Then and Now. In: *The Environment in Asia Pacific Harbours* edited by Wolanski E. Springer: Dordrecht, Netherlands, 293-307.

**Jose EC, Furio EF, Borja VM, Gatdula NC, Santos MD (2015)**. Zooplankton composition and abundance and its relationship with physico-chemical parameters in Manila Bay. *Oceanography* 3 136. doi:10.4172/2332-2632.1000136.

**Pokavanich T and Nadaoka K (2006)**. Three-dimensional hydrodynamics simulation of Manila Bay. Symposium on Infrastructure Development and the Environment 2006 , 7-8 December 2006, Seameo-Innotech University of the Philippines, Diliman, Quezon City, Philippines, 1-14.

**Poniente, J.A. and Santos MD (2017).** Preliminary Comparison of Remote Sensing-Derived Chlorophyll *a* Concentration and Sea Surface Temperature with the Fisheries Resources and Ecological

Data in Manila Bay. *Philippine Journal of Fisheries* **24**(1) 183-191. DOI: 10.31398/tpjf/24.1.2016A00011.

**Poquita-du RC and Todd PA (2015).** Understanding harmful algal bloom (HAB) occurrences in Manila Bay, Philippines, *Sustainability Matters*, 1-32. Doi: 10.1142/9789814719155_0002.

**PEMSEA (2007).** Manila Bay: Initial risk assessment. PEMSEA Technical Information Report No. 2007/01112 p. Global Environment Facility/United Nations Development Programme/ International Maritime Organization Regional Programme on Building Partnerships in Environmental Management for theSeas of East Asia PEMSEA), Quezon City, Philippines.

**Reyes T and Bedoya D (2008)**. Agrochemical use in the Philippines and its consequences to the environment, 12. Available: greenpeace.org.

**Roesler CS and Barnard AH (2013).** Optical proxy for phytoplankton biomass in the absence of photophysiology: Rethinking the absorption line height. *Methods in Oceanography* **7** 79–94. http://dx.doi.org/10.1016/j.mio.2013.12.003

**Rousseaux CS, and Gregg WW (2015).** Recent decadal trends in global phytoplankton composition. *Global Biogeochem. Cycles*, **29**, 1674–1688. doi:10.1002/2015GB005139.

**Roxy MK, Dasgupta P, McPhaden MJ, Suematsu T, Zhang C and Kim D (2019).** Twofold expansion of the Indo-Pacific warm pool warps the MJO life cycle. *Nature* **575** 647-651. doi: 10.1038/s41586-019-1764-4.

**Sathyendranath S, Brewin RJW et al. (2019)**. An ocean-colour time series for use in climate studies: the experience of the Ocean-Colour Climate Change Initiative (OC-CCI), *SENSORS*, ISSN 1424-8220 (online) 19 p. 4285, JRC117980. DOI: 10.3390/s19194285 (online).

**Siringan FP and Ringor CL (2007).** Changes in bathymetry and their implications on sediement dispersal and rates of sedimentation in Manila Bay. *Science Dilliman* **10**(2) 12-26.

**Sotto LPA, Beusen AHW, Villanoy CL, Bouwman LF and Jacinto GS (2015).** Nutrient Load Estimates for Manila Bay, Philippines using Population Data. *Ocean Science Journal* **50** (2) 467-474.

**Supa S, Kontar EA and Ishitobi T (2008)**. Groundwater discharge as an important land-sea pathway into Manila Bay, Philippines. *Journal of Coastal Research*, **24**(1A), 15–24.

**Sy AGA, Tobias ML, Borja VM, Gatdula NC, Santos, MD and Furio EF (2017).** Profile of salinity, temperature, heavy metal (Pb, Cd, Hg) and sediment Hydrogen sulfide concentration of Manila Bay, Philippines from 2012 to 2015. *Philippine Journal of Fisheries* **24**(1) 116-139. DOI: 10.31398/tpjf/24.1.2016A0008.

**Szekielda KH (2020a).** Significant Environmental Changes in the Northwest Indian Ocean: Warming Trend and Reduction of Chlorophyll. *International Journal of Geology, Earth and Environmental Sciences*, ISSN: 2277-2081, **10** (3), 56-68.

**Szekielda, KH (2020b).** Environmental changes in the South China Sea. *International Journal of Geology, Earth and Environmental Sciences*, ISSN: 2277-2081, **10**(2), 8-22.

**Szekielda KH and M. A. L. G. Guzman ALG (2021)**. Changes in the Philipppine coastal environment. *International Journal of Geology, Earth & Environmental Sciences*, ISSN: 2277-2081, Vol. II, 198-207.

**Taniguchi M, Burnett WC, Dulaiova H, Siringan, F, Foronda J, Wattayakorn G, Rung-**

**Tirado R and Bedoya D (2008).** Agrochemical use in the Philippines and its consequences to the environment. Available: greenpeace.org https://www.greenpeace.to/publications/gpsea_agrochemical-use-in-the-philip.pdf

**USAID (2017)**. Climate change risk in the Philippines: Country Fact Sheet, 5pp.

**Velasquez IB and Jacinto GS (1995)**. ASEAN criteria and monitoring: advances in marine environmental management and human health protection. *Proceedings in ASEAN-Canada Midterm Review*. Conference in Marine Science, Singapore, 278–284.

**Vergara JDD, Jose EC, Borja VM, Gatdula NC, Metillo EB, Santos MD and Furio EF (2017).** Effect of Nutrient Over-enrichment on Spatio-temporal Variability of Phytoplankton in Manila Bay, Philippines. *The Philippine Journal of Fisheries* **24** (1) 140-165.

DOI: 10.31398/tpjf/24.1.2016A0009.

**Villanoy CL, and Martin M (1997).** Modeling the circulation of Manila Bay: Assessing the relative magnitudes of wind and tide forcing. *Science Diliman* **9** 26-35.

**Wang SF, Tang DL, He FL, Fukuyo Y and Azanza RV (2008).** Occurrences of harmful algal blooms (HABs) associated with ocean environments in the South China Sea. *Hydrobiologia* **596** 79–93.

**World Data Atlas (2016).** Philippines **-** Fertilizer Consumption Per Unit Of Arable Land.